NANO LETTERS

2003
Vol. 3, No. 3
419−423

Hierarchical Pore Structure and Wetting Properties of Single-Wall Carbon Nanotube Fibers

Alexander V. Neimark,* Sigrid Ruetsch, Konstantin G. Kornev, and Peter I. Ravikovitch

Center for Modeling and Characterization of Nanoporous Materials, TRI/Princeton, P.O. Box 625, Princeton, New Jersey 08542

Philippe Poulin, Stéphane Badaire, and Maryse Maugey

Centre de Recherche Paul Pascal/CNRS, Université Bordeaux I, Avenue Schweitzer, 33600 Pessac, France

Received January 8, 2003; Revised Manuscript Received January 28, 2003

ABSTRACT

We show that single-wall carbon nanotube (SWNT) fibers produced by the particle-coagulation spinning process possess a well-developed hierarchical skin–core structure. Primary SWNTs are organized in bundles that are 10–30 nm in diameter. The nanotube bundles form elementary filaments, which constitute the fiber skin, and a highly porous nanofelt, which fills the fiber core. The elementary filaments of ∼0.2–2 μm diameter are well aligned along the fiber axis and densely packed. The hierarchical pore structure organization determines unique wetting and sorption properties of SWNT fibers. Experiments with capillary condensation and droplet absorption of wetting fluids agree with the proposed skin–core model and can be used for pore structure characterization. The well-developed porosity and high surface area in conjunction with controllable electrical and mechanical functionalities make the SWNT fibers attractive materials for nanotechnologies, where wetting and sorption properties play an important role.

Introduction. A simple particle-coagulation spinning (PCS) process has been recently proposed to produce continuous single-wall carbon nanotube (SWNT) fibers.[1] The PCS process[1,2] employs surfactant-enriched aqueous solutions of SWNTs. Mixed with an aqueous poly(vinyl alcohol) solution in a shearing hydrodynamic field, SWNTs align in the direction of flow, aggregate, and form ribbons, which are then pulled out of the bath and stretched into a high-density fiber. By contrast to composite fibers, where nanotubes are embedded in a polymeric matrix, the fibers produced by the PCS method consist of an interconnected network of polymer chains and SWNTs. The fibers can be freely stretched, twisted, knotted, or bent.[1] Mechanical properties of SWNT fibers and their potential applications for nanofiber-reinforced composites, actuators, electromagnetic shielding, emitters, microelectrodes, and so forth were discussed in refs 1−6.

In the present work, we demonstrate that SWNT fibers possess a hierarchical morphology with a well-developed porosity and a high surface area. This makes the SWNT fibers attractive materials for new types of nanofluidic devices, ad- and absorbents, catalysis support and host systems for the encapsulation of biomolecules, sensors, smart textiles, and other nanotechnologies in which wetting and sorption properties play an important role.[1−7] In this letter, we study sorption of vapors and liquids on SWNT fibers and establish relations between their wetting and structural properties.

Materials Preparation. SWNT fibers of 10−50 μm diameter were produced by the PCS method.[1,2] The samples were made from SWNT prepared by the electric arc discharge[8] or by the Hipco process.[9] In both cases, the initial nanotube dispersion was obtained by sonicating an aqueous solution of a few tenths of 1 wt % of SWNTs and about 1 wt % of sodium dodecyl sulfate (SDS). The suspension was injected into a rotating bath of a PVA solution as described in ref 1. The injection rate was 50 mL/h, the flow velocity of the PVA solution was 12.5 m/min, and the diameter of the spinneret was about 0.5 mm. The fibers were washed in pure water to desorb SDS and PVA partially. The fibers studied by the gas adsorption measurements (see below) were annealed at 320 °C in air during 3 h. This procedure allowed 95% of the remaining organic species to be removed while preserving the SWNT fibers intact.

To compare the adsorption properties of SWNT fibers, a sample of bucky paper was used as a reference material.[3]

* Corresponding author. E-mail: aneimark@triprinceton.org.

10.1021/nl034013x CCC: $25.00
Published on Web 02/14/2003

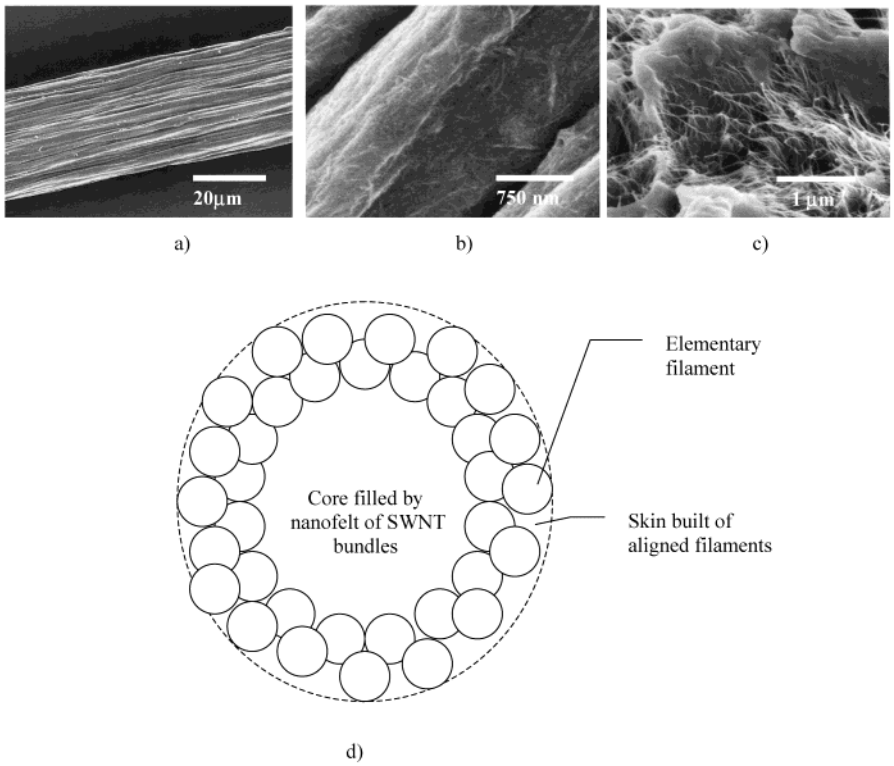

Figure 1. Hierarchical morphology of SWNT fibers. (a) Outer surface of fiber composed of aligned elementary filaments; (b) elementary filaments of 0.2−2 μm diameter built of packed SWNT bundles; (c) nanofelt of SWNT bundles of 10−30 nm diameter; and (d) skin−core model of a SWNT fiber.

Bucky paper was prepared by depositing a suspension of electric arc nanotubes onto a Teflon membrane filter. The nanotube mat deposited on the membrane was washed with pure water to remove SDS and was then dried. The sample of bucky paper had a thickness of about 25 μm.

Hierarchical Morphology of SWNT Fibers. The fiber morphology was studied by SEM. As shown in the SEM images presented in Figure 1, SWNT fibers possess a hierarchical structure with several levels of structural organization. A SWNT fiber of 10−50 μm diameter is composed of aligned straight elementary filaments. The filaments have a hairy surface. The elementary filaments of 0.2−2 μm diameter are built of densely aligned nanotube bundles. The nanotube bundles of 10−30 nm diameter are formed by primary SWNTs of 1−2 nm diameter.[4] Although the elementary filaments are aligned in a close-packed configuration constituting the fiber skin of 1−5 μm diameter, the fiber core consists of a nanofelt of loosely packed nanotube bundles.

The skin−core morphology of SWNT fibers resembles the skin−core model of polyacrylonitrile (PAN)-based carbon fibers.[10−12] This model is partially confirmed by an enlarged picture of a fracture cross section of a SWNT fiber (Figure 2a). It finds an indirect confirmation by the results of X-ray scattering and polarized Raman spectroscopy, which were used to characterize the nanotube orientation in SWNT fibers.[6,13,14] The orientation was characterized by the full width at half-maximum (fwhm) of the azimuthal Gaussian or Lorentzian intensity distributions. The smaller the fwhm, the better the nanotube orientation. In X-ray scattering

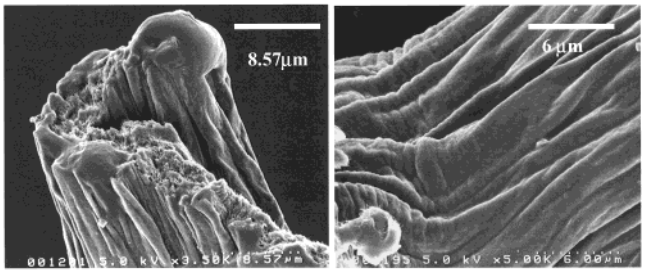

Figure 2. (a) Fracture (fiber was broken, not cut); (b) bend: kink bands that appear as buckling on the inside of the bent polymer fiber.

experiments, where the whole fiber was exposed to radiation, it was about 75°.[6,13] When measured with polarized Raman spectroscopy, where only a limited boundary layer (~1 μm) was probed, the fwhm was about 35°.[14] This difference was significant and reproducible. This observation agrees with the skin−core model: the nanotube alignment in the elementary filaments is more pronounced than in the nanofelt.

The hierarchical organization of SWNT fibers determines their unique properties. In particular, an exceptional bending ability can be explained if we hypothesize that the fiber skin is enriched by polymer. An examination of the SEM of fibers, which are either bent or knotted, shows a characteristic banding distributed over the folded region (Figure 2b). In response to a local compression, the filaments form kinks that take on the local stress, thus keeping the fiber core almost undeformable. With progressive deformation, the domains of individual kink bands propagate inwardly beneath the skin

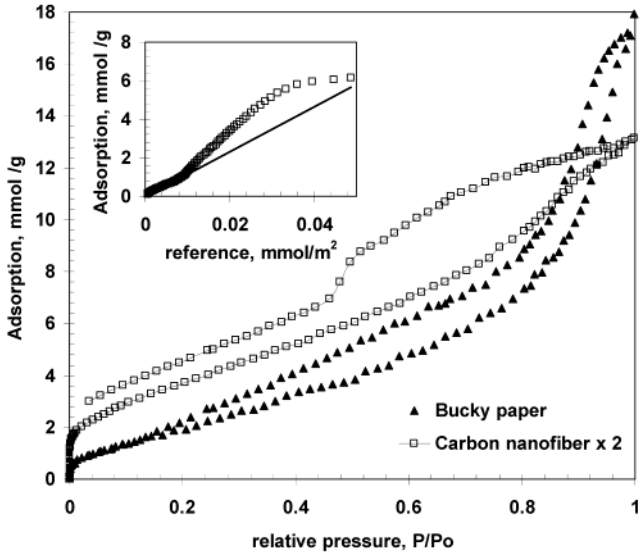

Figure 3. Adsorption−desorption isotherms on SWNT fibers and bucky paper. Note that the adsorption isotherm on SWNT fibers has been multiplied by 2 to avoid an overlap with the isotherm on bucky paper. The inset shows a comparison plot of the adsorption on SWNT fibers versus the reference nongraphitized carbon black.[19]

into the core, eventually causing the fiber rupture. This picture of fiber bending was suggested in ref 15 and proven for many polymer fibers.[16]

Adsorption and Absorption Properties of SWNT Fibers. The hierarchical pore structure of SWNT fibers determines their wetting and sorption properties and can be characterized by using adsorption and absorption experiments. We studied sorption and wetting properties of SWNT fibers by two methods: (i) capillary condensation[17] and (ii) droplet absorption.[18] The capillary condensation method probes the pore structure of the nanofelt core and within the elementary filaments in the range from 0.3 nm to ∼50 nm (maximum size of nanotube bundles). The droplet absorption method provides additional information about the transport pores of submicrometer sizes.

Capillary Condensation. The nanopore structure (<50 nm) and surface properties of SWNTs and bucky paper samples were studied by N_2 adsorption. Adsorption−desorption isotherms at 77.4 K were measured with the Autosorb-1C automated instrument (Quantachrome Corp.). The adsorption−desorption isotherms (Figure 3) form hysteresis loops that are typical of mesoporous solids. A plateau on the isotherms at relative pressures above $P/P_0 \approx 0.95$ indicates a well-defined upper limit of mesopore sizes, especially for the sample of SWNT fibers. Small hysteresis at low pressures is believed to be due to experimental errors because only a limited quantity of materials was available for volumetric adsorption measurements.

Comparison plots (see inset of Figure 3) showed that below the relative pressure $P/P_0 = 0.02$ the adsorption isotherms on SWNT fibers and bucky paper were similar to the reference isotherm on nonporous nongraphitized carbon black.[19] This similarity indicates the absence of micropores of size smaller than ∼1.5 nm, which is consistent with the fact that the primary nanotubes are closed. The fact that the surface properties of the SWNT fibers are akin to those of nongraphitized rather than graphitized carbons indicates the presence of impurities. The absence of narrow micropores is also evident from low BET surface areas S_{BET} and small values of the energetic C constant. For SWNT fibers, $S_{BET} = 160$ m^2/g and $C = 37$, and for bucky paper, $S_{BET} = 200$ m^2/g and $C = 15$.

The porosity of elementary filaments and nanofelt is associated with mesopores between nanotube bundles and, probably, some micropores within the bundles. Pore-size distributions were calculated from the adsorption isotherms using the NLDFT method for carbonaceous materials,[17] assuming a model of a slit-shaped pore with graphitic walls. Although this model does not reflect a complex geometry of pore channels in the material, the results of calculations can be considered to be reasonable estimates, which can be used for comparison with the pore-structure parameters of other carbonaceous adsorbents obtained with the same experimental and data treatment protocols. The calculated pore volume of SWNT fibers is about 0.2 cm^3/g, and the pore size ranges from ∼1.5 to ∼20 nm with a median value of ∼8 nm (Figure 4). This value is used below to estimate the capillary pressure associated with these pores. For bucky paper, the lower limit of the pore size is ∼2 nm, whereas the pore-size distribution is considerably broader and the pore volume is greater than ∼0.5 cm^3/g.

Droplet Absorption. To characterize the structure of macropores (100 nm/1 μm), we have applied the method of droplet absorption that was recently developed in ref 18. In absorption experiments, a droplet of a wetting liquid is placed on the fiber. During the process of droplet absorption, the droplet shape and volume are monitored by high-speed photography. The kinetics of fluid penetration is determined by the pore-structure morphology. We used hexadecane as a wetting liquid.

To interpret the absorption data, we employ the skin−core model for the fiber pore structure. The model implies that the thickness h of the fiber skin is appreciably smaller than the fiber radius R_f. The pores in the skin are divided into transport pores between the elementary filaments and sorption pores within the filaments between and inside nanotube bundles. The pores in the fiber core, which consists of the nanofelt of nanotube bundles, are expected to be more homogeneous. The size of the sorption pores in the nanofelt and in the elementary filaments is significantly smaller than the size of the transport pores. The upper estimate of the characteristic time of liquid penetration in the radial direction into the core, which is based on the Lucas−Washburn equation,[20,21] gives $t_{rd} \approx R_f^2\eta/\gamma R \approx 0.005$ s. Here, γ is the surface tension, η is the viscosity, and R is the characteristic radius of the pores in the nanofelt. Therefore, we may assume a uniform liquid saturation across the fiber cross section and a frontal liquid propagation along the fiber axis. The resistance to liquid flow through the nanofelt under an axial pressure gradient is very high. Thus, the liquid propagation in the axial direction is controlled by the rate of spreading of the droplet through the transport pores of the skin. The characteristic size, R, of the sorption pores in the nanofelt

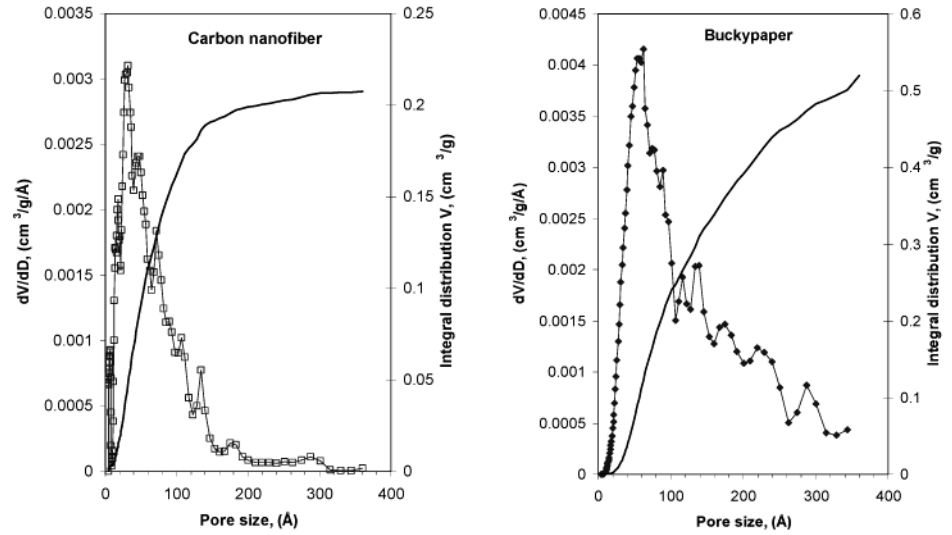

Figure 4. Pore-size distributions of SWNT fibers (left) and bucky paper (right) calculated by the NLDFT method.

and within the elementary filaments determines the driving capillary pressure.

To describe the kinetics of droplet spreading in the skin−core structure of SWNT fibers, we have modified the model of droplet absorption employed in the paper.[18] Therewith, at the late stage of droplet penetration, the kinetics of absorption is described by the Lucas−Washburn-type equation as

$$\frac{d\Delta V}{dt} = \frac{[2\epsilon_s \pi R_f h]^2 [1 + R_f\epsilon_c/(2h\epsilon_s)]2k\gamma \cos\theta}{\eta \Delta V R} \quad \text{or}$$

$$\Delta V = 4\epsilon_s \pi R_f h \sqrt{\left[1 + \frac{R_f\epsilon_c}{2h\epsilon_s}\right]\frac{k\gamma \cos\theta}{\eta R}t} \qquad (1)$$

Here, ϵ_s is the porosity associated with the interfilament pores of the skin, ϵ_c is the porosity of sorption pores in the nanofelt and elementary filaments, θ is the contact angle, k is the skin permeability, and $\Delta V = V - V_0$ is the difference between the current and initial droplet volumes. Note that the volume of sorption pores can be determined independently from capillary condensation data. The contact angle is defined by fitting the droplet profile onto the Carrol unduloid.[18,22] In our experiments with hexadecane, the contact angle was zero. The permeability was estimated by assuming that the filaments were closely packed to form a hexagonal elementary cell. Hence, $\epsilon = (\sqrt{3} - \pi/2)/\sqrt{3} \approx 0.1$ and $k = ar^2$, where r is the filament radius and constant $a \approx 0.003$ is taken from the exact equation for the resistance factor of a hexagonal elementary cell.[23]

Substituting into eq 1 the physical parameters for hexadecane $\eta = 3.3$ sp and $\gamma = 27$ dyn/cm and taking $R_f = 15$ μm and $r = 1$ μm, we obtain from the slope in Figure 5

$$h\sqrt{\left[\frac{1 + \frac{R_f\epsilon_c}{2h\epsilon_s}}{R}\right]} \approx 5 \text{ mm/mm}^{1/2}$$

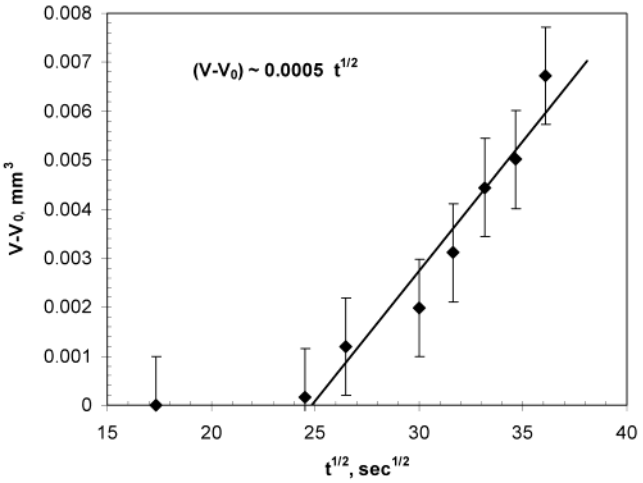

Figure 5. Lucas−Washburn kinetics of hexadecane absorption. Linear regression gives $V - V_0 = 0.0005t^{1/2} - 0.0132$; the regression coefficient is $Rg^2 = 0.9479$.

Thus, for skin thickness $h \approx 0.005$ mm, we have

$$R \approx \left[1 + \frac{R_f\epsilon_c}{2h\epsilon_s}\right] \text{nm}$$

Taking the density ρ of SWNT, which accounts for the voids in nanotubes $\rho = 1.25$ g/mL[24] and the sorption pore volume $V_p = 0.2$ cm^3/g, as determined by the capillary condensation, we estimate the porosity of sorption pores as $\epsilon_c = \rho V_p/(1 + \rho V_p) = 0.2$. Hence, the characteristic diameter of sorption pores is about 8 nm, in agreement with capillary condensation data. This analysis confirms the skin−core model of SWNT fibers.

Conclusions. In summary, the PCS method[1,2] provides a promising way to produce highly porous SWNT fibers with exceptional mechanical properties. SWNT fibers possess a hierarchical skin−core structure. Primary nanotubes form bundles of 10−30 nm diameter. Nanotube bundles are packed into straight cylindrical elementary filaments of 0.2−2 μm

diameter. Elementary filaments form the fiber skin, and the fiber core consists of a nanofelt of nanotube bundles. We showed that SWNT fibers are highly porous and capable of absorbing liquids and vapors in significant amounts. The isotherms of nitrogen vapor sorption and desorption form a hysteresis loop that is typical of mesoporous solids. An interpretation of the isotherms by the density function theory method shows that the porosity of the nanofelt and elementary filaments of SWNT fiber is about 0.2 cm^3/g and that the pore diameter ranges from ∼1.5 to ∼20 nm with a median of ∼8 nm. Fluid absorption by SWNT fibers was studied by the method of droplet absorption. An analysis of the absorption kinetics confirms the skin−core model. In particular, interfilament channels control the transport properties, and sorption pores in the nanofelt and elementary filaments determine the absorption capacity and the capillary pressure. The fibers produced by the particle-coagulation spinning of single-wall carbon nanotubes can be used as absorbing/adsorbing and reinforcing components of composite materials, membranes, and other nanostructures.

References

(1) Vigolo, B.; Penicaud, A.; Coulon, C.; Sauder, C.; Pailler, R.; Journet, C.; Bernier, P.; Poulin, P. *Science (Washington, D.C.)* **2000**, *290*, 1331.
(2) Poulin, P.; Vigolo, B.; Launois, P. *Carbon* **2002**, *40*, 1741.
(3) Baughman, R. H. *Science (Washington, D.C.)* **2000**, *290*, 1310.
(4) Baughman, R. H.; Zakhidov, A. A.; de Heer, W. A. *Science (Washington, D.C.)* **2002**, *297*, 787.
(5) Abramson, A. R.; Tien, C. L. *Microscale Thermophys. Eng.* **1999**, *3*, 229.
(6) Vigolo, B.; Poulin, P.; Lucas, M.; Launois, P.; Bernier, P. *Appl. Phys. Lett.* **2002**, *81*, 1210.
(7) Thiry, M. *AATCC Rev.* **2001**, *1*, 12.
(8) Journet, C.; Maser, W. K.; Bernier, P.; Loiseau, A.; de la Chapelle, M. L.; Lefrant, S.; Deniard, P.; Lee, R.; Fischer, J. E. *Nature (London)* **1997**, *388*, 756.
(9) Nikolaev, P.; Bronikowski, M. J.; Bradley, R. K.; Rohmund, F.; Colbert, D. T.; Smith, K. A.; Smalley, R. E. *Chem. Phys. Lett.* **1999**, *313*, 91.
(10) Bennett, S. C.; Johnson, D. J. *Carbon* **1979**, *17*, 25.
(11) Johnson, D. J. Carbon Fibers. In *Structure Formation in Polymeric Fibers*; Salem, D., Ed.; Hanser: Munich, 2000; p 329.
(12) Oya, N.; Johnson, D. J. *Carbon* **2001**, *39*, 635.
(13) Launois, P.; Marucci, A.; Vigolo, B.; Bernier, P.; Derre, A.; Poulin, P. *J. Nanosci. Nanotechnol.* **2001**, *1*, 125.
(14) Anglaret, E.; Righi, A.; Sauvajol, J. L.; Bernier, P.; Vigolo, B.; Poulin, P. *Phys. Rev. B* **2002**, *65*, art. no. 165426.
(15) Dobb, M. G.; Johnson, D. J.; Saville, B. P. *Polymer* **1981**, *22*, 960.
(16) *Structure Formation in Polymeric Fibers*; Salem, D., Ed.; Hanser: Munich, 2000.
(17) Ravikovitch, P. I.; Vishnyakov, A.; Russo, R.; Neimark, A. V. *Langmuir* **2000**, *16*, 2311.
(18) Chen, X.; Kornev, K. G.; Kamath, Y. K.; Neimark, A. V. *Text. Res. J.* **2001**, *71*, 867.
(19) Kruk, M.; Jaroniec, M.; Gadkaree, K. P. *J. Colloid Interface Sci.* **1997**, *192*, 250.
(20) Lucas, R. *Kolloid-Z.* **1918**, *23*, 15.
(21) Washburn, E. W. *Phys. Rev.* **1921**, *17*, 273.
(22) Carroll, B. J. *J. Colloid Interface Sci.* **1976**, *57*, 488.
(23) Kacimov, A. R.; Kayumov, I. R. *J. Porous Media* **2002**, *5*, 199.
(24) Murata, K.; Kaneko, K.; Kokai, F.; Takahashi, K.; Yudasaka, M.; Iijima, S. *Chem. Phys. Lett.* **2000**, *331*, 14

NL034013X